DOI 10.1007/s11041-024-01072-8
Metal Science and Heat Treatment, Vol. 66, Nos. 7 – 8, November, 2024 (Russian Original Nos. 7 – 8, July – August, 2024)

UDC 621.793.79

IMPACT OF ELECTRON BEAM TREATMENT ON THE STRUCTURE AND PHASE COMPOSITION OF TiB_2 – Ag COATING DEPOSITED BY ELECTRICAL EXPLOSION SPRAYING ON A COPPER SUBSTRATE

A. D. Filyakov,[1] V. V. Pochetukha,[1] D. A. Romanov,[1] E. S. Vashchuk,[2] and V. E. Gromov[1]

Translated from *Metallovedenie i Termicheskaya Obrabotka Metallov*, No. 8, pp. 13 – 21, August, 2024.

Original article submitted April 4, 2024.

The microstructure of a new TiB_2 – Ag metal matrix composite coating deposited by electrical explosion spraying and modified by electron beam treatment is studied using x-ray diffraction analysis and scanning and transmission electron microscopy. It is shown that the phase composition of the coating depends on the deposition mode, and the subsequent electron beam treatment normalizes it. The main phases of the resulting modified coating are Ag, TiB_2 and B_2O. After the electron beam treatment, the microstructure of the coating transforms. The nanostructure of the silver matrix is transformed into a nanocrystalline structure with an average crystal size of tens to hundreds of nanometers.

Key words: electrical explosion spraying, electron beam treatment, microstructure, phase composition, silver, titanium diboride.

INTRODUCTION

Moving electrical contacts play a key role in provision of safety of recent power service systems [1]. Development of automation systems enhances the demand for gages and sensors containing electrical contacts. The safety of such systems depends largely on the fail-safe operation of the sensors [2]. This makes elevation of the properties of electrical contact materials an importance task of the science of materials.

The key feature of electrical contact materials is the combination of high electrical conductivity, thermal conductivity, hardness and oxidation resistance. These materials include composite silver-based alloys used in low-voltage switches [3]. Pure silver possesses relatively high thermal and electrical conductivities at low mechanical properties and erosion resistance [4]. These disadvantages are eliminated by adding various materials to silver [1]. In contrast to the alloys, silver virtually does not dissolve in the hardening (second) phase of metal matrix composites. As a result, these phases preserve their thermal and electrical properties [5]. The silver matrix in such materials provides heat and electrical conduction, while the hardening phase improves the mechanical properties, and raises the adherence (the weldability) and the erosion resistance.

Electrical contact materials of the CdO – Ag system have found wide application due to the combination of low cost and high operating properties [7, 8]. However, the European ecological legislation limits their use because of the negative action of cadmium oxide on human health and on environment [9]. Consequently, this oxide is inadmissible for novel safe electrical contact materials [10]. There are numerous alternative silver-based variants like SnO_2 – Ag, ZnO – Ag and others. However, the electrical contact materials of the SnO_2 – Ag system have poor processibility, low electrical conductivity at high temperatures, and relatively high contact resistance [10]. Electrical contact materials of the ZnO – Ag system exhibit higher adherence and contact wear [11].

It seems appropriate to develop silver electrical contact materials with additions of titanium diboride TiB_2. This compound has a high melting temperature (over 2900°C) and a hardness of 30 GPa at the lowest resistivity among the superhard ceramics (9 $\mu\Omega \cdot cm^2$) [12].

Coatings based on silver with titanium diboride can be deposited on copper contacts by electrical explosion spraying, which is a variant of plasma spraying. In electrical explosion spraying, the coating is deposited due to rapid heat-

[1] Siberian State Industrial University, Novokuznetsk, Russia (e-mail: filyakov.1999@mail.ru).
[2] Branch of the Gorbachev Kuzbass State Technical University, Prokopyevsk, Russia.

ing and electrical explosion of a conductor under the action of high currents. The dynamic shock wave created as a result, sprays the products of the electrical explosion onto the surface of the sample and produces a coating [13, 14]. The method has some restrictions and disadvantages. The metallic conductor has to be made of a thin foil, a wire, or a fine dispersed powder for rapid heating and explosion. To obtain composite coatings by the method of electrical explosion spraying, we should create thicker compound conductors from several layers of a foil and a powder. The increase in the thickness of the conductor limits the heating and causes an asynchronous explosion yielding coarse hard particles of various sizes [15], which results in instability of the structure and of the properties of the coatings. To homogenize the structure and the properties, we can resort to a treatment with pulsed electron beams.

The aim of the present work was to study the effect of electron beam treatment on the structure and phase composition of TiB_2 – Ag coatings deposited onto a copper surface by the method of electrical explosion spraying.

METHODS OF STUDY

The coating was sprayed onto a copper substrate with the help of an EVU 60/10 M electrical explosion setup. The setup consists of a charging device, a capacitive energy storage system, and a plasma accelerator. The operation and the design of the setup is described in detail in [16].

The electrical explosion during the spraying of the coating provided a power density of 5.5 GW/m^2 during the heat impact on the irradiated surface. The pressure in the shock-compressed layer near the irradiated surface was about 12.5 MPa, the pressure of the residual gases in the working chamber was about 100 Pa, the plasma temperature at the outlet from the nozzle was about 10^4 K, and the duration of the pulse was about 100 μsec.

The composite electrical explosion conductor consisted of a silver foil with the following chemical composition (in wt.%): 99.9 Ag, 0.058 Cu, 0.035 Fe, 0.003 Pb, 0.002 Sb, and 0.002 Bi. TiB_2 powder with a mass of 200 mg was placed onto the central part of the foil. After the electrical explosion spraying, the samples were subjected to a pulsed electron beam in a "Solo" device [14]. The modes of the electron beam treatment (EBT) of the samples are presented in Table 1.

The structure and the elemental composition of the coating were studied with the help of a KYKY-EM6900 scanning electron microscope. The elements were determined by the method of energy dispersive x-ray spectroscopy (EDS). The structure was analyzed using a JEM-2100F JEOL transmission electron microscope at a distance $h = 200 – 1000$ nm from the surface of the sample after the electrical explosion spraying and at a distance $h = 200 – 23{,}500$ nm after the electron beam treatment.

The diffraction studies were performed using a DRON-8N x-ray diffractometer equipped with a parabolic mirror on the primary beam and a position-sensitive detector Mythen 2R ID (640 channels; the size of one strip 50 μm). The accelerating voltage supplied to the x-ray tube was 40 kV; the current was 20 mA. The specimens were not rotated. The identification of the phase composition, the qualitative and quantitative phase analyses, and the structure studies were made using the "CDA – Crystallography and Diffraction Analysis" software with an incorporated file of powder standards (AO ITS "Burevestnik", version 2023-01-24-144022.8dec10c0f).

TABLE 1. Modes of Electron Beam Treatment (EBT) of TiB_2 – Ag Coatings

Mode	j, J/cm^2	τ_b, μsec	N	q, sec^{-1}
1	45	50	30	0.3
2	50	200	30	0.3
3	60	200	30	0.3
4	70	200	30	0.3

Notations: j) beam energy density; τ_b) duration of beam action; N) number of pulses; q) pulse frequency.

RESULTS AND DISCUSSION

Figure 1 presents the diffraction patterns of TiB_2 – Ag from three samples of coatings (*1-1*, *1-2*, *1-3*) deposited by the method of electrical explosion spraying (without subsequent EBT). The reflections detected correspond to Cu_2O, Ag, TiB, TiB, Ag, Cu_4Ti_3, Cu, AgTi, B_2O_3 and B_2O phases. It can be seen that the coatings differ in the phase compositions.

Sample *1-1* contains two phases of copper oxide (*1* and *2*) with the same crystal lattice but different parameters of the elementary cell (Fig. 1*a*). This difference can be associated with the nonequilibrium conditions of the deposition of the coatings explainable by different rates and different physicochemical parameters of the particles of the heterogeneous plasma flow formed under the electrical explosion (Table 2). It should be noted that the phase parameters differ substantially from the standard values. Sample *1-2* also contains a copper oxide. In addition, there is a copper phase corresponding to the substrate (Fig. 1*b*).

Sample *1-3* has a phase composition different from those of samples *1-1* and *1-2*. Copper and copper-containing phases have not been detected. The dominant phase in the coating is B_2O_3 oxide (Fig. 1*c*) and its concentration attains 65 wt.%.

Figure 2 presents the structure in cross section and the elemental composition of the TiB_2 – Ag coating deposited by the electrical explosion method onto a copper substrate. The coating consists of a silver matrix with randomly arranged inclusions of TiB_2. The average size of the particles fluctuates from 3.64 to 3.44 μm, which corresponds to the fineness of the powder used for the spraying. Coarse inclusions of

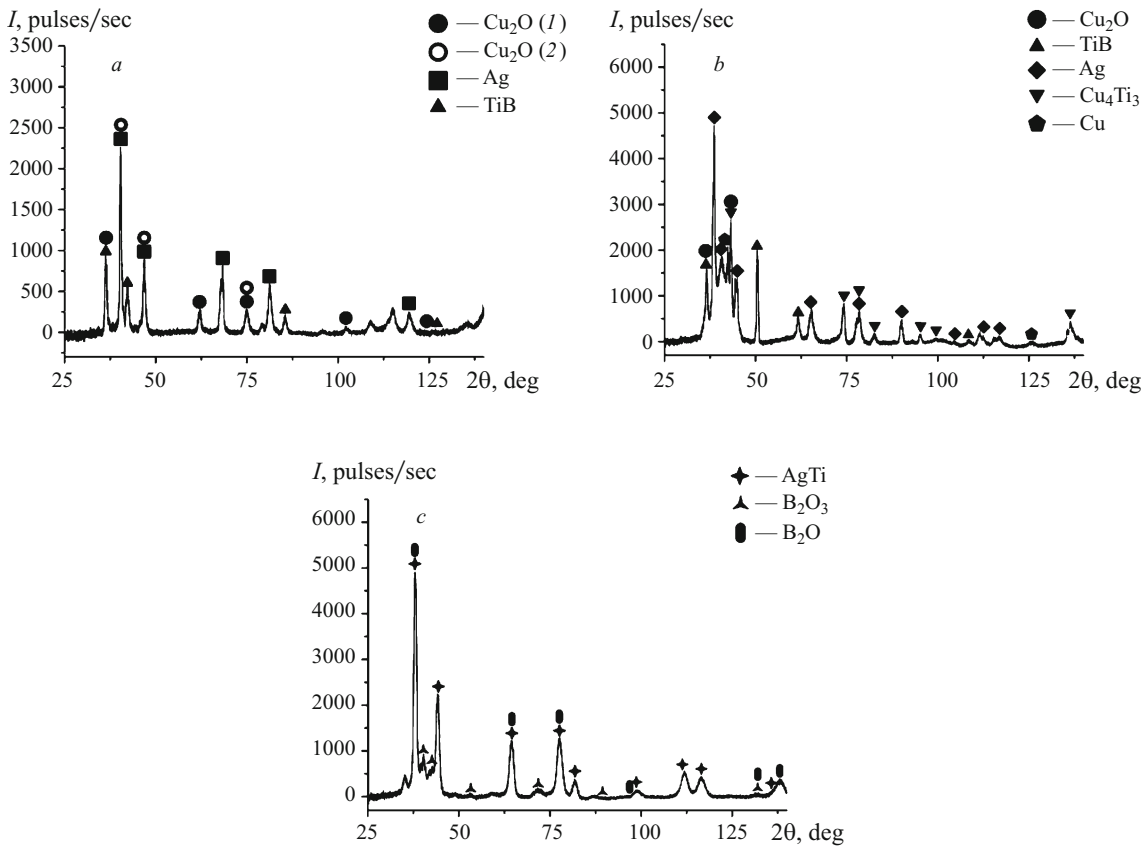

Fig. 1. X-ray diffraction patterns from samples *1* (*a*), *2* (*b*) and *3* (*c*) with TiB_2 – Ag coatings sprayed by different modes of electrical explosion.

TABLE 2. Parameters of Phases Detected in TiB_2 – Ag Coatings Deposited by Electrical Explosion Spraying without EBT

Sample	Phase	C_{ph}, wt.%	Lattice constant, Å	CSR, nm
1-1	Cu_2O (*1*)	48	a = 4.2856	24
	Cu_2O (*2*)	15	a = 4.2017	15
	Ag	37	a = 2.7459 c = 6.7269	22
	TiB	Traces	–	–
1-2	Cu_2O	29	a = 4.2474	28
	TiB	23	a = 4.2560	17
	Ag	20	a = 4.0420	13
	Cu_4Ti_3	16	a = 3.1256 c = 19.7407	25
	Cu	12	a = 3.6138	41
1-3	AgTi	8	a = 2.8778 c = 8.1387	16
	B_2O_3	65	a = 4.2370 c = 8.3950	11
	B_2O	27	a = 2.8968 c = 7.0080	17

Notations: C_{ph}) content of the phase; CSR) coherent scattering regions.

TiB_2 with a size of 10 – 15 μm form in the silver matrix as a result of fusion of two-five particles. The clusters with an average size of over 30 μm are agglomerates of coarse inclusions and individual particles. The volume of the coating contains pores with an average size of 3.5 μm. They have appeared as a result of chipping of TiB_2 particles during preparation of the cross sections.

The microstructure of the silver matrix is presented in Fig. 3*a*. It bears numerous pores with an average size of 0.36 μm formed as a result of the nonequilibrium crystallization conditions [17, 18]. Some of the pores have consolidated into coarser formations with a size of about 2 μm in the regions with reduced cooling rate and low content of dissolved gas due to the nonequilibrium conditions of the deposition of the coatings.

Figure 4 presents the microstructure and the maps of the distribution of elements in the coating layer located at distance h = 200 – 1000 nm from the surface. It can be seen that the microstructure consists of different layers with a thickness of 450 – 600 nm based on the silver matrix. Layer I contains an inclusion in the form of a TiB_2 particle with fused boundaries. Layers I and II also contain a Ti band and a B inclusion; their concentration grows toward layer III. These data show that the particles of TiB_2 under the electrical ex-

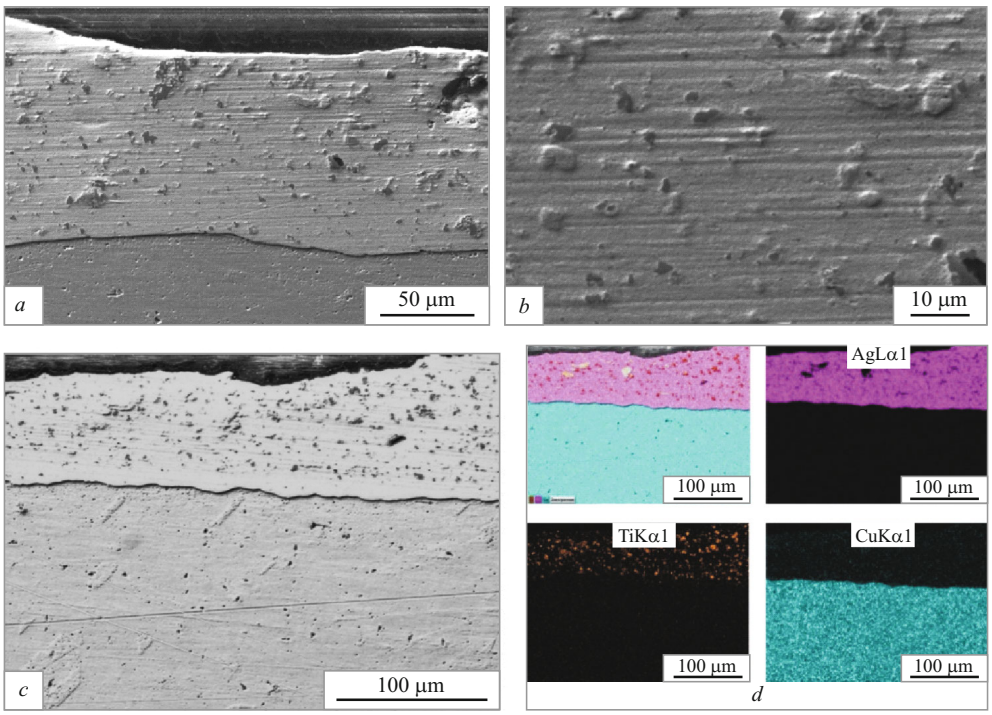

Fig. 2. Structures (SEM) of a TiB_2 – Ag coating deposited by electrical explosion spraying onto a copper substrate (*a*, *c*) and of a silver matrix with inclusions of TiB_2 (*b*) and maps of distribution of Ag, Ti and Cu atoms (EDS) (*d*).

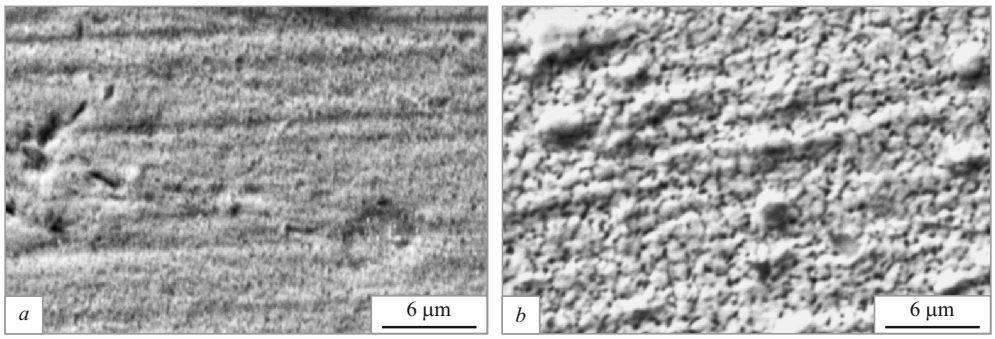

Fig. 3. Structure (SEM) of the silver matrix of a TiB_2 – Ag coating obtained by electrical explosion spraying before (*a*) and after (*b*) electron beam treatment.

plosion spraying can remain steady in the silver matrix or interact with the silver producing new compounds.

The considerable differences in the phase compositions of the coatings are connected with the physical laws of formation of coatings in electrical explosion spraying. In this process, the conductor composed of the foil and of the powder heats and explodes yielding numerous particles differing in the size and in the phase state. The particles are affected by the shock wave arising due to the explosion. The heterogeneous plasma flow formed as a result collides with the surface of the substrate and then propagates in all directions covering the whole of the surface [19].

In the initial stage of the spraying, the flow of the heterogeneous plasma consists of two zones, i.e., a high-speed jet with low density and a high-density disc moving at a low speed. Therefore, the thermal impact on the surface meets a nonmonotonic time dependence, i.e., has two maximums due to the actions of the high-speed plasma jet and of the low-speed plasma disc. This circumstance is responsible for such an impact of the heat flows onto the surface that the plasma of the high-speed jet fuses the surface and the plasma with condensed particles of the high-speed disc saturates the molten metal of the bottom layer. Thus, the modified layers acquire unique graded structures [20]. The initial positions and the shape of the powder component on the foil influence the formation of the plasma flow and the phase composition of the coating obtained.

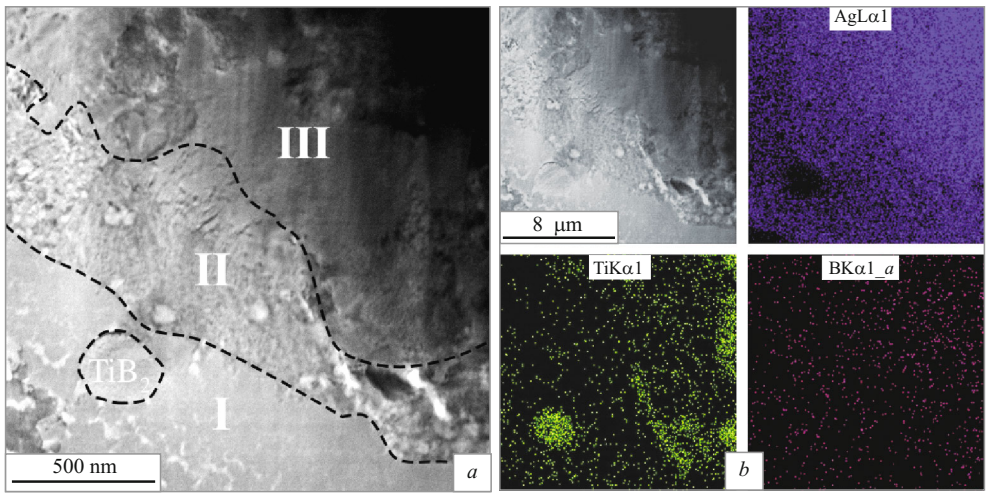

Fig. 4. Structure (TEM) of a TiB_2 – Ag coating obtained by electrical explosion spraying at a distance of 200 – 1000 nm (*a*) and maps of distribution of Ag, Ti and Cu atoms (EDS) (*b*).

To determine the changes in the phase composition after the EBT, we made an x-ray phase analysis of the coatings. Figure 5 presents the phase compositions of coatings on four samples subjected to different modes of EBT. It can be seen that their compositions differ from those without EBT. The samples after the EBT contain TiB, Ag, Cu, Cu_2O, Ti, B_2O, TiB_2, and Cu_2Ti.

The reflections between the main silver peaks in the diffraction patterns of sample *2-3* are manifested more than those of sample *2-1* but less than those of sample *2-2*. The phase composition of sample *2-4* differs substantially from those of samples *2-1* – *2-3*. The diffraction pattern from sample *2-4* exhibits wide silver reflections and narrow reflections of the other phases.

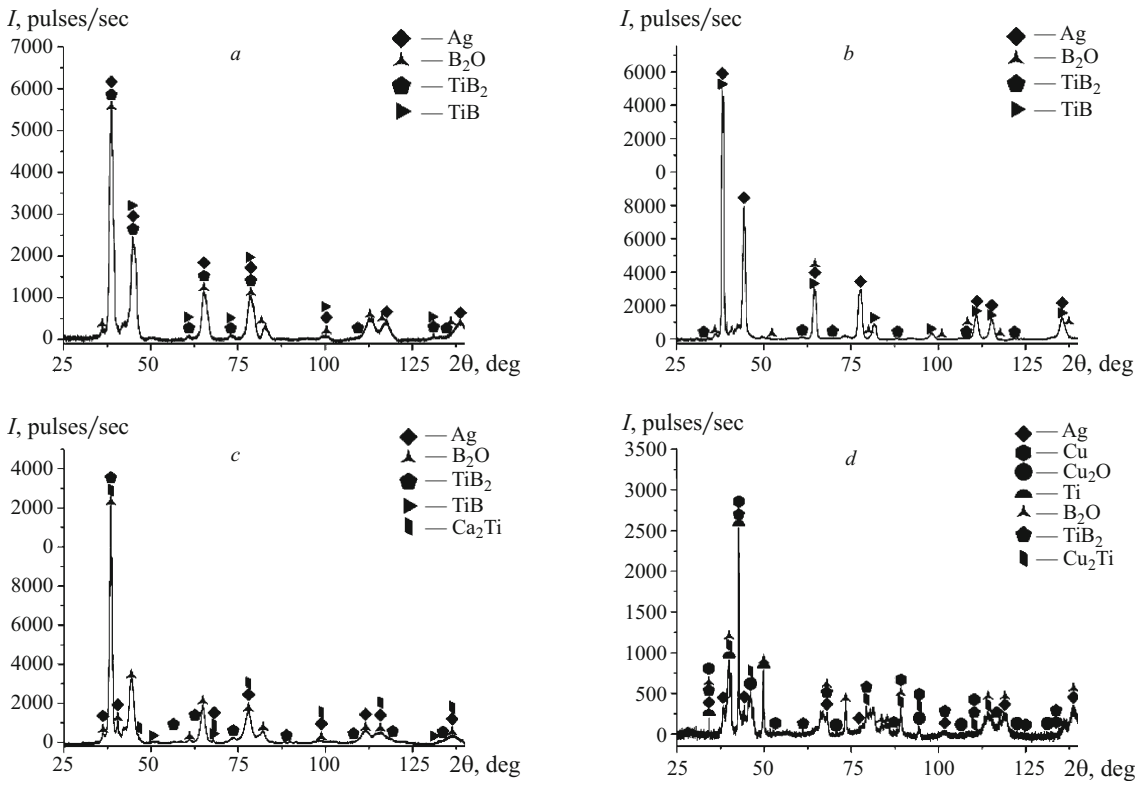

Fig. 5. X-ray diffraction patterns from samples *2-1* (*a*), *2-2* (*b*), *2-3* (*c*) and *2-4* (*d*) with a TiB_2 – Ag coating modified by electron beam treatment.

TABLE 3. Parameters of Phases in TiB_2 – Ag Coatings after EBT

Sample	Phase	C_{ph}, wt.%	Lattice constant, Å	CSR, nm
2-1	Ag	56	$a = 4.0324$	13
	B_2O	21	$a = 2.8857$; $c = 7.0292$	55
	TiB_2	20	$a = 3.0342$; $c = 3.2272$	15
	TiB	3	$a = 6.1221$; $b = 3.0746$; $c = 4.5616$	32
2-2	Ag	43	$a = 4.0779$	42
	B_2O	24	$a = 2.8549$; $c = 7.1524$	73
	TiB_2	25	$a = 3.0535$; $c = 3.2618$	38
	TiB	8	$a = 6.0308$; $b = 2.9703$; $c = 4.6600$	24
2-3	Ag	33	$a = 4.0847$	26
	B_2O	19	$a = 2.8760$; $c = 7.0389$	89
	TiB_2	11	$a = 3.0398$; $c = 3.2564$	44
	TiB	27	$a = 6.0200$; $b = 3.0393$; $c = 4.4600$	19
	Cu_2Ti	10	$a = 7.9616$; $b = 4.4701$; $c = 4.2696$	20
2-4	Ag	22	$a = 4.0047$	15
	Cu	12	$a = 3.6927$	58
	Cu_2O	8	$a = 2.8164$; $c = 12.8000$	18
	Ti	15	$a = 2.9571$; $c = 4.7613$	40
	B_2O	30	$a = 2.8655$; $c = 7.0138$	32
	TiB_2	7	$a = 3.0107$; $c = 3.1778$	45
	Cu_2Ti	6	$a = 7.9453$; $b = 4.3780$; $c = 4.2663$	25

Notations: C_{ph}) content of the phase; CSR) coherent scattering regions.

It can be seen from Table 3 that increase in the energy and in the time of the electron beam pulse reduces the content of the Ag phase and elevates the concentrations of the TiB, Ti, B_2O and TiB_2 refractory phases. The presence of

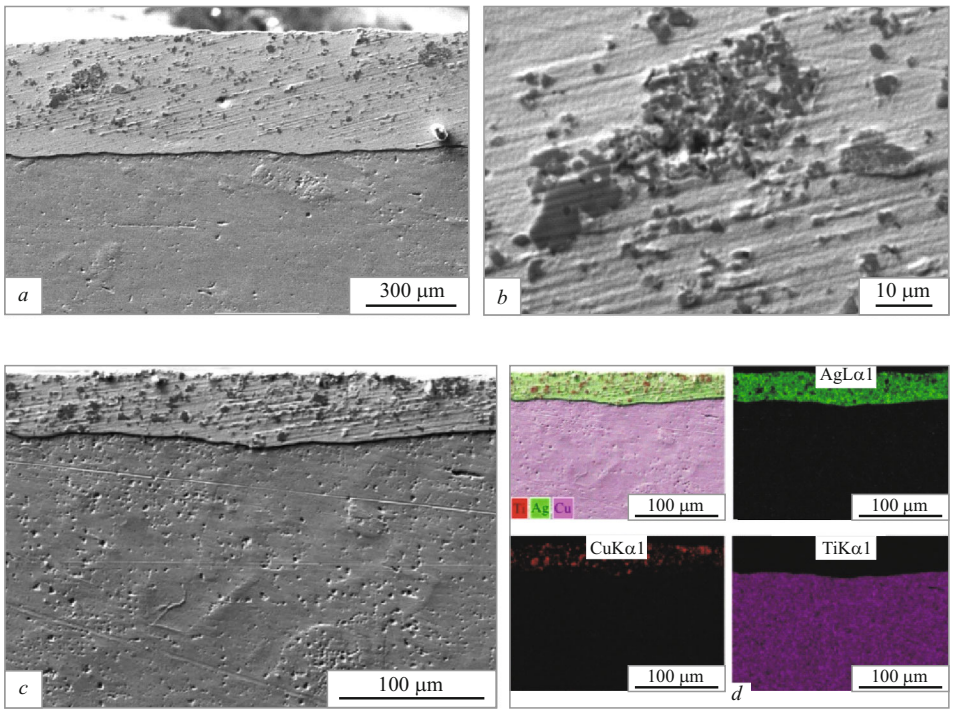

Fig. 6. Structures (SEM) of a TiB_2 – Ag coating modified by electron beam treatment and of the copper substrate (*a*, *c*), silver matrix with TiB_2 – Ag cluster (*b*), and maps of distribution of Ag, Ti and Cu atoms (EDS) (*d*).

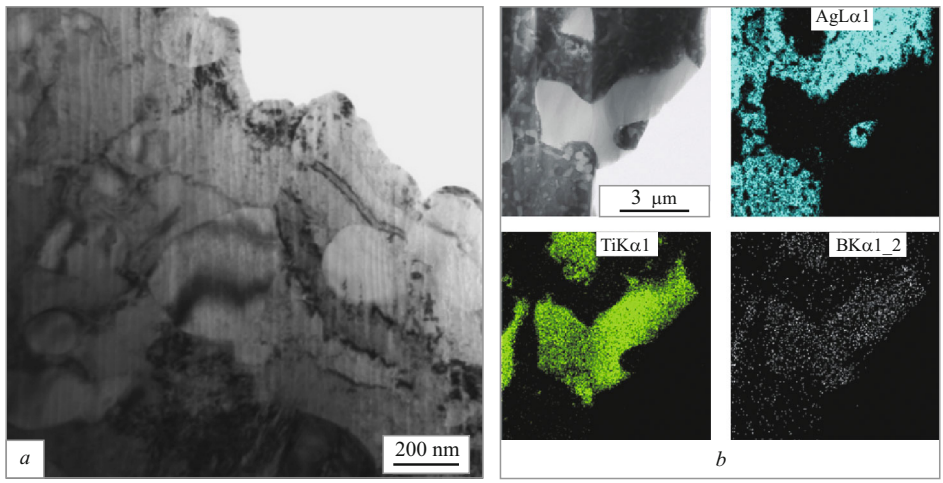

Fig. 7. Structure (TEM) of the electron-beam-modified layer in a TiB_2 – Ag coating located at a distance of 200 nm – 23.5 μm from the surface (*a*) and maps of distribution of Ag, Ti and Cu atoms obtained by EDS (*b*).

copper-containing phases in samples *2-3* and *2-4* may indicate excess evaporation of the silver matrix and melting of the copper substrate under the action of the electron beam. It can be inferred that treatment modes *3* and *4* cause degradation of the coating.

Figure 6 presents the cross sectional structure and the maps of the distribution of the elements in a coating of the TiB_2 – Ag system after EBT. After the EBT, the thickness of the coating is 12 – 14% less at the same structure, but the content of clusters and coarse inclusions is higher. The large voids in the coating become smaller. The size range of the TiB_2 particles reduces to 2.88 – 3.21 μm.

Figure 3*b* presents the microstructure of the silver matrix of a coating after the EBT. The small pores formed as a result of the electric explosion spaying are replaced by a cellular structure. Such a structure can form on the surface of a melt due to development of capillary instability arising by a thermal capillary mechanism [21]. Similar structures have been observed earlier on the surface and in the surface layer of irradiated aluminum alloys [22].

Figure 7 presents the structure and the maps of the distribution of elements in a layer located at a distance of 200 – 23,500 nm from the surface. The layer is represented by nanosize grains with different morphologies and a size varying from tens to hundreds of nanometers. The rapid cooling in the EBT leaves a short time for the grains to grow. The results of the EDS show that the grains contain Ag, Ti and B atoms and are surrounded by dislocation lines. The dislocation density in the layer is high. The grains in the layer are accompanied by fused TiB_2 particles with an average size of about 1.5 μm

CONCLUSIONS

We have studied coatings of the TiB_2 – Ag system deposited by the method of electrical explosion spraying onto a copper substrate and subjected to four modes of electron beam treatment. After the electron beam treatment, the phase composition of the coating does not change substantially. The main phases in the modified coating are Ag, TiB_2 and B_2O. When the energy density and the duration of the action of the electron beam are increased, the content of the highly fusible Ag phase decreases and the contents of the refractory B_2O and TiB_2 phases increases. The heating and melting of the copper substrate due to the excess energy of the electron beam also produces copper-containing Cu, Cu_2O and Cu_2Ti phases. The structure of the cross section represented by a silver matrix and TiB_2 inclusions remains virtually invariable. However, the average size of the TiB_2 particles decreases to 2.88 – 3.21 μm. The thermal capillary instabilities caused by the electron beam treatment produce a cellular structure in the silver matrix of the coating. The modified layers acquire a nanostructure with nanosize grains of different morphologies and fused particles of TiB_2.

DECLARATIONS

Acknowledgments

The authors gratefully acknowledge the participation of the Laboratory of Electron Microscopy and Image Processing of SibSIU.

Funding

This work has been funded by the Russian Science Foundation (grant No. 22-79-10012), https://rscf.ru/project/22-79-10012/.

Credit Authorship Contribution Statement

A. D. Filyakov: conceptualization, writing of original draft, preparation of graphical materials; *V. V. Pochetukha*:

formal analysis, validation of results; *D. A. Romanov*: editing of original draft, acquisition of funding; *E. S. Vashchuk*: formal analysis, investigation; *V. E. Gromov*: project administration.

Declaration of Competing Interest

The authors confirm that they have no known financial or interpersonal conflicts that would have appeared to have an impact on the research presented. We are approving the final version of the manuscript.

Availability of Data and Material

Data will be made available on request.

Code Availability

Not applicable.

Supplementary Information

Not applicable.

REFERENCES

1. R. Grieseler, M. K. Camargo, M. Hopfeld, et al., "Copper-MAX-phase composite coatings obtained by electro-co-deposition: A promising material for electrical contacts," *Surf. Coat. Technol*., **321**, 219 – 228 (2017). DOI: 10.1016/j.surfcoat.2017.04.060
2. J. Song, H. Yuan, and V. Schinow, "Fretting corrosion behavior of electrical contacts with tin coating in atmosphere and vacuum," *Wear*, **426 – 427**, 1439 – 1445 (2019). DOI: 10.1016/j.wear.2018.11.024
3. C. Wu, Q. Zhao, N. Li, et al., "Influence of fabrication technology on arc erosion of $Ag/10SnO_2$ electrical contact materials," *J. Alloys Compd*., **766**, 161 – 177 (2018). DOI: 10.1016/j.jallcom.2018.06.317
4. Z. Zhou, T. Zhao, Y. Feng, et al., "Arc erosion characteristics evolution of Ag/Ti_3SiC_2 composites during repetitive arc breakdowns in SF_6 gaseous medium," *Int. J. Appl. Ceram. Technol*., **18**, 1716 – 1724 (2021). DOI: 10.1111/ijac.13727
5. N. Ray, B. Kempf, T. Mützel, et al., "Effect of WC particle size and Ag volume fraction on electrical contact resistance and thermal conductivity of Ag – WC contact materials," *Mater. Des*., **85**, 412 – 422 (2015). DOI: 10.1016/j.matdes.2015.07.006
6. M. T. Kesim, H. Yu, Y. Sun, et al., "Corrosion, oxidation, erosion and performance of Ag/W-based circuit breaker contacts: A review," *Corros. Sci*., **135**, 12 – 34 (2018). DOI: 10.1016/j.corsci.2018.02.010
7. C. Yangfang, Y. Xiaofang, B. Xiaoping, et al., "Research on the influence of different oxide particles on properties of AgCdO contact material," *J. Phys. Conf. Ser.*, **1948**, 012192 (2021). DOI: 10.1088/1742-6596/1948/1/012192
8. X. Wang, H. Yang, M. Chen, et al., "Fabrication and arc erosion behaviors of $AgTiB_2$ contact materials," *Powder Technol*., **256**, 20 – 24 (2014). DOI: 10.1016/j.powtec.2014.01.068
9. O. Nilsson, F. Hauner, and D. Jeannot, "Replacement of AgCdO by $AgSnO_2$ in DC contactors," in: *Proceed. 50th IEEE Holm Conf. on Electrical contacts and 22nd Int. Conf. on Electrical Contacts, Seattle, WA, USA, 23 – 23 September* (2004), pp. 70 – 74.
10. S. M. Senthil, R. Parameshwaran, R. Rathanasamy, and K. S. Praveen, "Fabrication of a novel silver-based electrical contact composite and assessment of its mechanical and electrical properties," *Arch. Metall. Mater.*, **66**, 1087 – 1094 (2021).
11. V. Ćosović, N. Talijan, D. Živković, et al., "Comparison of properties of silver-metal oxide electrical contact materials," *J. Min. Metall. B*, **48**, 131 – 141 (2012).
12. X. Wang, G. Li, J. Zou, et al. "Investigation on preparation, microstructure, and properties of $AgTiB_2$ composite," *J. Compos. Mater.*, **45**, 1285 – 1293 (2011). DOI: 10.1177/0021998310376100
13. H. Tamura, M. Konoue, and A. B. Sawaoka, "Zirconium boride and tantalum carbide coatings sprayed by electrothermal explosion of powders," *J. Therm. Spray Technol*., **6**, 463 – 468 (1997). DOI: 10.1007/s11666-997-0032-6
14. N. N. Koval and Y. F. Ivanov, "Nanostructuring of surfaces of metalloceramic and ceramic materials by electron-beams," *Russ. Phys. J*., **51**, 505 – 516 (2008). DOI: 10.1007/s11182-008-9073-7
15. C. Li, J. Feng, W. Yuan, et al., "Discharge characteristics and dynamic process of directional spraying binary and ternary alloy coating via electrical explosion method," in: D. Dai, C. Zhang, Z. Fang, and X. Lu (eds.), *Proceed. 4th Inter. Symp. on Plasma and Energy Conversion, Foshan, China, 14 – 16 October, 2022*, Springer Nature, Singapore (2023), pp. 302 – 311. DOI: 10.1007/978-981-99-1576-7 29
16. D. A. Romanov, "Improving die tooling properties by spraying TiC – Ti – Al and TiB_2 – Ti – Al electro-explosive coatings," *Mater. Res. Express*, **7**(4), 045010 (2020). DOI: 10.1088/2053-1591/ab86f6
17. D. Romanov, S. Moskovskii, S. Konovalov, et al., "Improvement of copper alloy properties in electro-explosive spraying of ZnO – Ag coatings resistant to electrical erosion," *J. Mater. Res. Technol*., **8**, 5515 – 5523 (2019). DOI: 10.1016/j.jmrt.2019.09.019
18. M. Vlasova, M. Kakazey, P. A. M. Aguilar, et al., "TiN – TiB_2 ceramics degradation in the region of a steady-state laser heating," *Surf. Coat. Technol*., **378**, 124738 (2019). P. 124738. DOI: 10.1016/j.surfcoat.2019.06.058
19. Q. Liu, T. Wang, Y. Bai, et al., "Formation mechanism of gas phase in supersonic atmospheric plasma sprayed NiCr – Cr_3C_2 cermet coatings," *Surf. Coat. Technol*., **397**, 126052 (2020). P. 126052. DOI: 10.1016/j.surfcoat.2020.126052
20. D. A. Romanov, S. V. Moskovskii, A. M. Glezer, et al., "Phase composition, structure, and wear resistance of electric-explosive CuO – Ag system coatings after electron beam processing," *Bull. Russ. Acad. Sci. Phys*., **83**, 1270 – 1274 (2019). DOI: 10.3103/S1062873819100174
21. V. Sarychev, S. Nevskii, S. Konovalov, and A. Granovskii, "Modeling of the initial stages of the formation of heterogeneous plasma flows in the electric explosion of conductors," *Curr. Appl. Phys*., **18**, 1101 – 1107 (2018). DOI: 10.1016/j.cap. 2018.06.010
22. D. A. Romanov, E. A. Budovskikh, Y. D. Zhmakin, and V. E. Gromov, "Surface modification by the EVU 60/10 electro-explosive system," *Steel Transl*., **41**, 464 – 468 (2011). DOI: 10.3103/S0967091211060131